Indian Journal of Engineering & Materials Sciences
Vol. 23, June 2017, pp. 187-193

# Effect of fiber orientation and ply stacking sequence on buckling behaviour of basalt-carbon hybrid composite laminates

S B Dhuban[a], S Karuppanan[a]*, A N Mengal[a,b] & S S Patil[a,c]

[a]Department of Mechanical Engineering, Universiti Teknologi PETRONAS, 32610 Bandar Seri Iskandar, Perak, Malaysia

[b]Balochistan University of Information Technology, Engineering and Management Sciences, Airport Road, Quetta, Pakistan

[c]Department of Mechanical Engineering, Manipal University Jaipur, 303 007, Jaipur, India

*Received 5 October 2015; accepted 8 March 2017*

The aim of this study is to investigate the effect of fiber orientation and ply stacking sequence of basalt-carbon hybrid composite laminates on the critical buckling strength, experimentally and by using nonlinear finite element analysis. The composite laminated plates are simply supported and subjected to axial compression load. Nonlinear FEA results using ANSYS have good agreement with the experimental results. FEA results showed that the outer layers have the most significant influence on the buckling strength of the composite laminated material. Furthermore, placing carbon fiber reinforced layers in the outer surface of the basalt-carbon/epoxy hybrid laminates results in significant increase in the critical buckling load compared to placing basalt fiber reinforced layers in the outer surface. It is also concluded that $[0_2C/0B/\pm 45B]_s$ laminate is the best combination of the hybrid stacking sequences as far as buckling strength is concerned.

**Keywords**: Buckling, Hybrid composite, Basalt fiber, Nonlinear FEA

The use of polymer matrix composites is continuously increasing in various conventional and advanced industries due to their superior mechanical properties. Polymer matrix composites have high specific strength and stiffness. These composites are corrosion and environment resistant and easy to fabricate at beneficial price[1]. Polymer matrix composites offer interesting design flexibility which makes it preferred in many applications. However, thin laminated composite structures often fail due to buckling loading. Hence, buckling analysis of thin laminated composites is necessary. The fiber combination which can resist buckling is desirable.

Basalt fiber which is relatively a newcomer in polymer matrix composites has shown great mechanical properties compared to common polymer matrix composites[2-5]. Moreover, it is significantly cheaper than carbon fibers and available in abundance in the earth's crust. Although very few studies are available in the literature, but manufacturers claim basalt fiber as an alternate of glass and carbon fiber because of its extraordinary properties. Burgoyne *et al.* [4] reported that the mechanical properties of basalt fiber are better compared to glass fiber. Velde *et al.*[5] compared the thermal properties of basalt fiber with glass fiber. They observed that basalt fiber can be used over a wide range of temperatures as compared to glass fibers. Wang *et al.*[6] studied that the interface formed between basalt fiber/epoxy resin was better than glass fiber/epoxy resin. Cziga´ny[7] investigated basalt fiber as the reinforcement in concrete matrix and asserted that the cheap basalt fibers can be efficiently applied in hybrid composite systems. Lopresto *et al.*[8] analyzed the mechanical properties of E-glass and basalt fiber reinforced plastic laminates. The experimental results showed a high performance of basalt fiber in terms of Young's modulus, compressive and bending strength, impact force and energy.

Several studies have been conducted to investigate the laminated composite structures considering their buckling and post buckling behavior under several loading and working conditions. Most of the studies are focused on the buckling behavior of glass fiber and E-glass reinforced plastics. Baz and Chen[9] studied the lateral buckling characteristics of flexible composite beams. They concluded that the buckled

*Corresponding author
(E-mail: saravanan_karuppanan@utp.edu.my)

beams can be brought back completely to their unbuckled configuration by proper activation of the shape memory effect. Demirci *et al.*[10] studied the Charpy impact behaviors of ±6 layered basalt and glass fiber reinforced epoxy composite pipe. They observed that the delamination damage in glass fiber reinforced composites was more dominant than in basalt fiber reinforced composites. Another Charpy based experimental study was carried out by Farsani *et al.*[11] to investigate the impact response of basalt fiber reinforced epoxy and basalt fiber metal laminate. This work also showed the usefulness of basalt and its mechanical impact strength. Thompson *et al.*[12] studied the post buckling behavior of laminated plate structures under the influence of a uniaxial load. They concluded that out-of-plane displacement of the post buckled laminates can be significantly reduced even for a small volume fraction. Ro and Baz[13] studied the static and buckling characteristics of flexible fiberglass reinforced composite plates. They concluded that the fibers are pre-tensioned and activated to generate significant phase recovery forces in order to increase the critical buckling load of the reinforced plates. Shukla *et al*.[14] concluded that the buckling strength of laminated plate is significantly influenced by material properties such as modulus of elasticity, plate aspect ratio and stacking sequence. Critical buckling load is also significantly affected by mixed boundary conditions[15].

Another important variable in the critical buckling load is the aspect ratio of the laminate. The maximum buckling load tends to decrease with increasing aspect ratio[15-17]. Fiber orientation has significant influence on the strength of the composite laminate. Fiber glass epoxy laminates having $0^{\circ}$ fiber orientation on the outer surface sustain higher buckling loads than laminates with $90^{\circ}$ orientation on the outer surface[18].

In recent years there has been a great interest in hybrid materials. The combination of basalt fiber with carbon fiber is the most recent and advanced area of hybrid technologies. Chikhradze *et al.*[19] proposed the use of hybrid epoxy composites reinforced by carbon, basalt and E-glass fibers for the manufacturing of wind turbines. Basalt-carbon/epoxy hybrid composite with alternate stacking sequence have been developed by Zhang *et al*.[20] to improve the toughness properties of conventional carbon reinforced composites. The experimental results confirmed that the hybrid composites containing basalt fibers displayed 46% higher open-hole compressive strength than that of plain carbon fiber composites. Also, various numerical studies have shown new advancements in the field of hybrid composites, especially basalt based laminate composites[21-23]. However, very little research is available in the literature that is related to buckling analysis of basalt fiber.

The aim of the present study is to investigate the effect of fiber orientation and ply stacking sequence on the critical buckling load of simply supported basalt-carbon/epoxy composite laminates experimentally and by using nonlinear finite element analysis (FEA) using ANSYS software.

## Experimental Procedure

### Materials

Basalt fiber (300 g/m$^2$ unidirectional, 450 g/m$^2$ woven) and carbon fiber (300 g/m$^2$ unidirectional) were supplied by Suretex Composite International China. The epoxy used was epocast (Bisphenol) and the curing agent was amine based epoharden (cycloaliphatic amine). Both epocast and epoharden was supplied by Portal Trading Malaysia. The mechanical properties of unidirectional basalt/epoxy and carbon/epoxy lamina are given in Table 1[24].

### Specimen preparation

Seven symmetrical lamination stacking sequences with eight layers of unidirectional 0° and biaxial +45° were selected for the current study. One eight-layered unidirectional 0° fiber layup of pure carbon fiber and one eight-layered unidirectional $0^{o}$ fiber layup of pure basalt fiber were used as a reference. The purpose of selecting a symmetrical lamination sequence was to avoid unpredictable wrap deflection and to reduce the problem of strain coupling. Therefore, symmetric composite laminates were prepared according to stacking sequences that are commonly used in wind turbine blade manufacturing as shown in Table 2.

Laminated composite plates were prepared using conventional hand lay-up method. The

Table 1 — Mechanical properties of unidirectional basalt/epoxy and carbon/epoxy lamina[24]

| Properties | Basalt/Epoxy | Carbon/Epoxy |
|---|---|---|
| $E_x$ (GPa) | 30.2 | 74.7 |
| $E_y$ (GPa) | 5.2 | 4.7 |
| $E_z$ (GPa) | 5.2 | 4.7 |
| $\upsilon_{xy}$ | 0.2 | 0.48 |
| $\upsilon_{yz}$ | 0.21 | 0.47 |
| $\upsilon_{xz}$ | 0.21 | 0.47 |
| $G_{xy}$ (GPa) | 2.05 | 21.5 |
| $G_{yz}$ (GPa) | 3.6 | 1.45 |
| $G_{xz}$ (GPa) | 3.6 | 21.5 |

plates were then cured for 24 h at room temperature as shown in Fig. 1. Since the fiber volume content has a significant effect on the strength of composite laminates, attempt was made to produce laminates with the same fiber volume fraction content. The standard ASTM D3171-11 "Constituent Content of Composite Materials" was used to determine the fiber volume fraction, weight and void content. Procedure G (Matrix burn off in a muffle furnace) of method 1 in the standard was used for constituent content determination. For each stacking sequence, three specimen samples were cut for the measurement of density and fiber volume fraction. Density of each specimen was determined in accordance to test methods D792. The samples were then put in a desiccated pre-weighed crucible and placed into a preheated muffle furnace at 565°C for 2 to 3 h to completely burn off the matrix and leave the reinforcements. After burning off, the specimens were allowed to cool at room temperature. Then the reinforcements were weighed to determine the fiber volume fraction. The fiber volume fraction and matrix volume fraction are calculated by using Eqs (1) and (2).

Table 2 — Specimen characteristics for buckling test

| Laminate code | Stacking sequence | Fiber orientation |
|---|---|---|
| C1 | $C_8$ | $[0_8C]$ |
| C2 | $C_2B_4C_2$ | $[0_2C/\pm 45B/0B]_S$ |
| C3 | $C_2B_4C_2$ | $[0_2C/0B/\pm 45B]_S$ |
| C4 | $C_2BC_2BC_2$ | $[0_2C/\pm 45B/0C]_S$ |
| B1 | $B_8$ | $[0_8B]$ |
| B2 | $B_2C_4B_2$ | $[0_B/\pm 45B/0_2C]_S$ |
| B3 | $B_2C_4B_2$ | $[\pm 45B/0B/0_2C]_S$ |
| B4 | $BC_2B_2C_2B$ | $[\pm 45B/0_2C/0B]_S$ |
| B5 | $BC_2B_2C_2B$ | $[\pm 45B/0_2C/\pm 45B]_S$ |

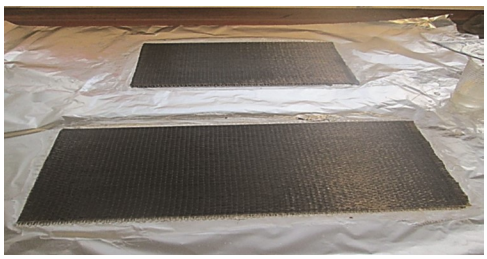

Fig. 1 — Laminated composite plates

Fiber volume fraction,

$$V_f = M_f / M_i \times 100 \times \rho_c / \rho_r \quad \ldots (1)$$

Matrix volume fraction,

$$V_m = (M_i - M_f) / M_i \times 100 \times \rho_c / \rho_m \quad \ldots (2)$$

where $M_i$, $M_f$, $\rho_c$, $\rho_r$ and $\rho_m$ represent the initial mass of the specimen in grams, final mass of the specimen after digestion or combustion in grams, density of the specimen in g/cm$^3$, density of the reinforcement in g/cm$^3$ and density of the matrix in g/cm$^3$, respectively. The void content is defined as,

$$V_c = 100 - (V_f + V_m) \quad \ldots (3)$$

The average fiber volume fraction content obtained by matrix ignition test was between 35% and 38%. Specimens were cut from the prepared plate using a diamond saw before they were sanded to remove any imperfection. The dimensions of the specimens are 400 mm × 40 mm × 3.2 mm in length, width and thickness, respectively as shown in Fig. 2.

**Testing procedure**

The experiment was conducted using strut buckling apparatus as shown in Fig. 3. The specimens were

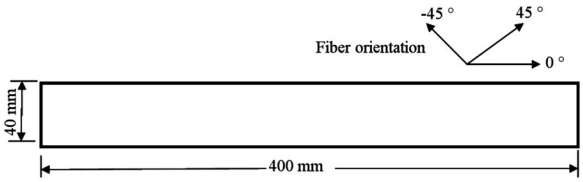


Fig. 2 — Dimensions of the specimen

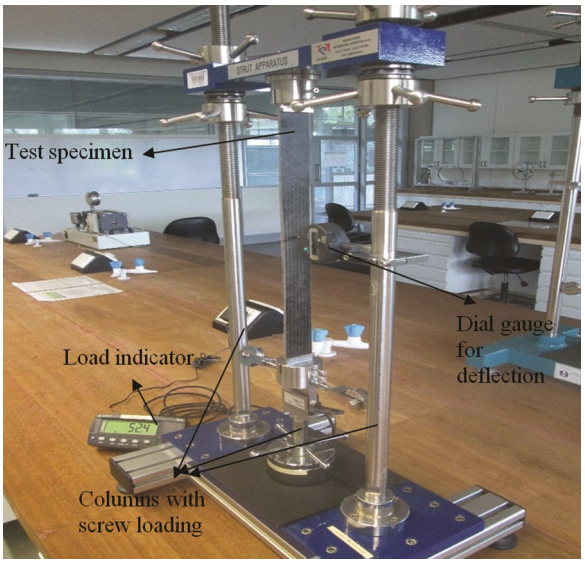


Fig. 3 — Buckling apparatus

loaded by step increments of 20 N each. The load and the corresponding mid-span deflection were recorded. The slope of the best fit line of the scatter points of the deflection versus deflection-load ratio as shown in Fig. 4 represents the critical buckling load (N). This approach minimizes the error in the calculation of critical buckling load. Three different specimens were tested for each stacking sequence.

## Nonlinear Finite Element Analysis Procedure

Nonlinear buckling analysis is a static analysis through which we can incorporate the nonlinearities due to loading, supports and the end conditions. In other words, nonlinear buckling analysis is a simulation procedure that allows for large deformations and geometrical and/or material nonlinearities. This type of analysis is the second step after a linear (or eigenvalue) buckling analysis approach. Generally, the buckling load obtained from a linear buckling analysis is higher than the true buckling load of a structure. The reason behind this is that there are no imperfections included in a linear buckling analysis, which are present during experimental testing[25]. Modelling of composites laminates using finite element analysis either by ANSYS or ABAQUS has been reported elsewhere[21-23]. In this study, similar numerical procedure as reported in literature to study nonlinear buckling analysis has been employed[26-28] for the modelling of basalt/epoxy composite laminates. The laminates were modelled similar to the test specimens (ASTM standards).

SHELL281 element type was used for the meshing of composite laminates, as it is suitable for analyzing thin to moderately-thick shell structures and for large strain nonlinear analyses. This element type has 8 nodes with 6 degrees of freedom at each node:

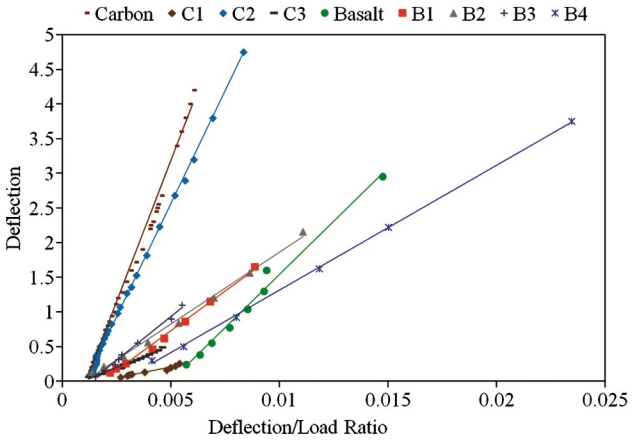


Fig. 4 — Deflection versus deflection-load ratio of laminates

translations in the x, y and z axes and rotations about the x, y and z axes. Furthermore, it supports modelling of composite shells efficiently[29].

Nonlinear FE buckling analysis is simply an extension of eigenvalue buckling analysis. To run a nonlinear buckling analysis, first it is necessary to run a linear eigenvalue buckling analysis to get the theoretical buckling limit as well as the first buckling mode of the structure. After the eigenvalue buckling analysis is complete, a nonlinear buckling analysis is performed. The key steps for successful nonlinear buckling analysis are given as:

### *Update the geometry*

A fraction of the first buckling mode of the linear eigenvalue buckling analysis is included as an input into the nonlinear buckling analysis to superimpose imperfection into the geometry to persuade the structure to buckle. Typically, 1% - 10% of the first buckling mode is included as an input into the nonlinear analysis.

### *Load application*

To make sure that the nonlinear buckling is captured, load that is slightly larger than the theoretical eigenvalue buckling limit should be applied to the structure.

### Effect of fiber orientation

The effect of the fiber orientation on the critical buckling load of basalt/epoxy composite laminates was studied using four-layer symmetric laminates. The following orientations were used: $[\theta/0^\circ]_s$, $[0^\circ/\theta]_s$,$[\theta/30^\circ]_s$,$[30^\circ/\theta]_s$,$[\theta/45^\circ]_s$,$[45^\circ/\theta]_s$, $[\theta/90^\circ]$ and $[90^\circ/\theta]_s$. The θ layer was varied from 0° to 90° while keeping the other layers constant.

### Effect of ply stacking sequence

The effect of ply stacking sequence (Table 2) on the critical buckling load of basalt-carbon/epoxy hybrid composite laminates was investigated through eight-layer symmetric laminates.

## Results and Discussion

### Effect of fiber orientation

The effect of fiber orientation on the critical buckling load of a four-layer symmetric basalt/epoxy composite laminated plate was studied using nonlinear FEA. Table 3 shows the critical buckling loads of different fiber orientations. Figures 5 and 6 show the nonlinear deflection versus load curve and the buckled shape of the composite laminated FE

Table 3 — Critical buckling loads of different fiber orientations

| | Critical buckling load (N) | | | | | | | |
|---|---|---|---|---|---|---|---|---|
| θ | [θ/0] | [0/θ] | [θ/90] | [90/θ] | [θ/30] | [30/θ] | [θ/45] | [45/ θ] |
| 90 | 15.32 | 55.44 | 8.61 | 8.61 | 8.90 | 8.82 | 10.02 | 12.70 |
| 80 | 15.22 | 55.39 | 8.53 | 8.61 | 8.77 | 8.72 | 9.89 | 12.58 |
| 70 | 15.02 | 55.30 | 8.43 | 8.56 | 8.42 | 8.46 | 9.45 | 12.00 |
| 60 | 15.05 | 55.33 | 8.82 | 8.90 | 8.33 | 8.33 | 9.07 | 11.24 |
| 50 | 16.19 | 55.72 | 10.72 | 9.53 | 9.58 | 8.66 | 9.76 | 10.94 |
| 40 | 20.20 | 56.70 | 15.59 | 10.61 | 14.03 | 9.66 | 13.43 | 11.45 |
| 30 | 28.98 | 58.26 | 24.24 | 12.05 | 23.14 | 11.24 | 22.08 | 12.92 |
| 20 | 42.03 | 60.02 | 36.30 | 13.59 | 36.14 | 13.02 | 35.45 | 14.94 |
| 10 | 55.58 | 61.45 | 49.21 | 14.83 | 49.26 | 14.46 | 49.40 | 16.78 |
| 0 | 62.00 | 62.00 | 55.44 | 15.32 | 55.33 | 14.05 | 56.13 | 17.69 |

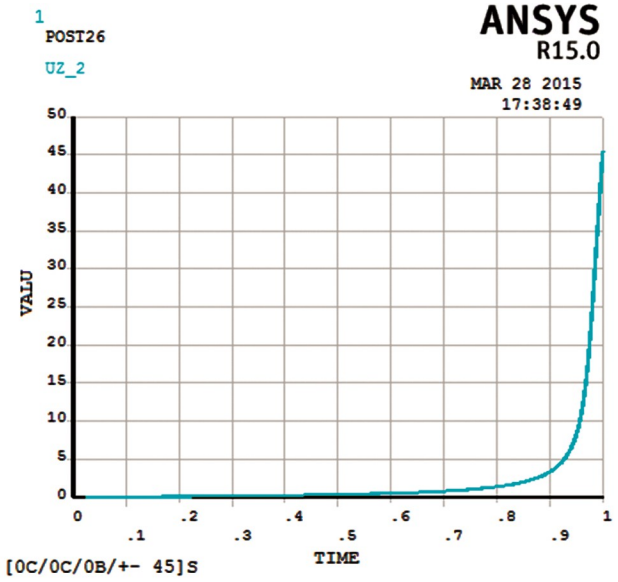


Fig. 5 — Nonlinear deflection versus load curve of composite laminated FE model

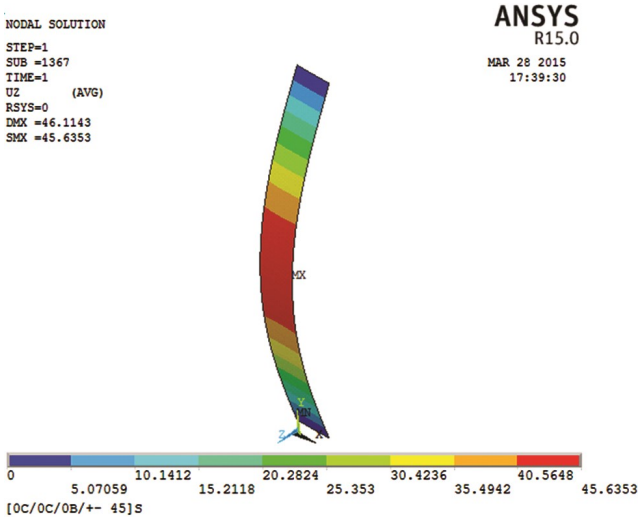


Fig. 6 — Buckled shape of composite laminated FE model

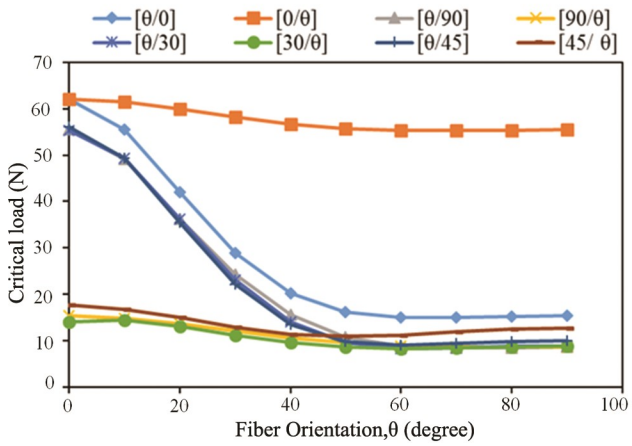


Fig. 7 — Critical buckling load versus fiber orientation

model, respectively. Figure 7 shows the graph of critical buckling load versus fiber orientation. It is very clear from the results that when the outer layer is kept constant whilst the fiber orientation of the inner layer is varied from 0° - 90°, the critical buckling load does not change much. However, if the inner layer is kept constant whilst the fiber orientation of the outer layer is varied from 0° - 90°, the critical buckling load decreases rapidly until θ value of 50°, after that the critical buckling load is almost constant. This indicates that the orientation of the outer layer plays a more significant role in the load carrying capability of the laminate.

Furthermore, when the outer layer is oriented in the zero direction, the variation of the critical buckling load is small regardless of the orientation of the inner layer. All stacking sequences achieved their highest critical buckling load at θ value of 0°. This result is similar as found by Jawad *et al*.[30] Moreover, the highest critical buckling load was achieved by $[0°/0°]_s$ laminate. The fiber orientation angle is measured relative to the applied load. 0° fiber orientation is parallel to the applied load. $[0°/0°]_s$ is the best fiber

orientation as far as buckling strength is concerned because all layers are oriented in the load direction which enhances the buckling strength of the laminate.

**Effect of ply stacking sequence**

Table 4 shows the nonlinear FEA critical buckling load of pure and hybrid composite laminates. Nonlinear FEA results show that pure carbon fibers reinforced epoxy oriented in 0° direction has higher critical buckling load than that of basalt fibers reinforced epoxy oriented in the same direction. This is due to the high longitudinal stiffness of carbon fibers. Hybrid laminates with carbon fiber reinforcement layers oriented in the 0° direction in the outer surface and basalt fibers reinforced layers on the inner surface have high critical buckling loads.

The buckling loads of these laminates are even comparable to that of pure carbon fiber reinforcement. That is due to the fact that the outer layers carry most of the buckling load. $[0°_{2C}/0°_{B}/ \pm 45°_{B}]_S$ laminate has higher buckling strength than $[0°_{2C}/ \pm 45°_{B}/0°_{C}]_S$ laminate despite the fact that $[0°_{2C}/\pm 45°_{B}/0°_{C}]_S$ has six carbon fibers reinforced layers compared to only four carbon fibers reinforced layers in $[0°_{2C}/0°_{B}/ \pm 45°_{B}]_S$ laminate. The reason is that the third layer of $[0°_{2C}/0°_{B}/ \pm 45°_{B}]_S$ laminate is oriented in the 0° direction compared to the $\pm 45°_{B}$ in $[0°_{2C}/\pm 45°_{B}/0°_{C}]_S$ laminate. The buckling strength of $[0°_{2C}/\pm 45°_{B}/0°_{C}]_S$ is higher compared to$[0°_{2C}/\pm 45°_{B}/0°_{B}]_S$ due to the fact that it contained 2 extra carbon layers in the middle.

$[\pm 45_{B}/0_{2C}/0_{B}]_S$ laminate has higher buckling strength compared to $[\pm 45_{B}/0_{2C} /\pm 45_{B}]_S$ laminate due to the fact that $[\pm 45_{B}/0_{2C} /0_{B}]_S$ laminate contains basalt in the 0° direction as the inner layer compared to $\pm 45°_{B}$in $[\pm 45_{B}/0_{2C} /\pm 45_{B}]_S$ laminate. The buckling strength of $[0_{B}/\pm 45_{B}/0_{2C}]_S$ laminate is higher than $[\pm 45_{B}/0_{B}/02_{C}]_S$ laminate because it has basalt in the 0° direction as the outer layers compared to $\pm 45°_{B}$ as the outer layers in the latter.

Table 4 — Critical buckling load of pure and hybrid laminates

| Group | Laminate code | Critical buckling load (N) | Critical stress, $\sigma_{cr}$ (MPa) |
|---|---|---|---|
| Pure laminates | B1 | 189 | 1.48 |
| | C1 | 474 | 3.70 |
| Hybrid laminates with carbon fibers in the outer layers | C2 | 428 | 3.34 |
| | C3 | 437 | 3.41 |
| | C4 | 432 | 3.38 |
| Hybrid laminates with basalt fibers in the outer layer | B2 | 186 | 1.45 |
| | B3 | 132 | 1.03 |
| Hybrid laminates with basalt fibers in the outer and inner layers | B4 | 221 | 1.73 |
| | B5 | 216 | 1.69 |

**Finite element analysis and experimental results comparison**

The results of the nonlinear FEA were validated using experimental results. Table 5 shows a comparison between the two methods. The percentage difference less than 10% between the FEA results and the experimental results is considered to be acceptable[31]. The results showed that all the nine laminates have results difference of less than 10%. Several factors may contribute to the differences in the results of the FEA and the experiment such as the variation of the thickness of the real specimen, the interfacial bond between the fiber and matrix phases and fiber volume fraction. Even though, the nonlinear FEA presented in this work includes geometrical nonlinearities, high variation in the thickness of the specimen could result in some percentage error between the numerical and experimental results. The efficiency of load transfer between the matrix and fiber depends on the interfacial bond. Thus, the weak interfacial bond will result in low buckling load. Furthermore, the fiber volume fraction obtained from

Table 5 — Numerical and experimental critical buckling load comparison

| Group | Laminate code | Critical buckling load (N) | | Critical stress, $\sigma_{cr}$ (MPa) | | Percentage difference (%) |
|---|---|---|---|---|---|---|
| | | FEA | Experimental | FEA | Experimental | |
| Pure laminates | B1 | 189 | 184 | 1.48 | 1.44 | 2.7 |
| | C1 | 474 | 460 | 3.70 | 3.59 | 3.0 |
| Hybrid laminates with carbon fibers in the outer layers | C2 | 428 | 398 | 3.34 | 3.11 | 7.5 |
| | C3 | 437 | 402 | 3.41 | 3.14 | 8.7 |
| | C4 | 432 | 400 | 3.38 | 3.13 | 8.0 |
| Hybrid laminates with basalt fibers in the outer layer | B2 | 186 | 170 | 1.45 | 1.32 | 9.4 |
| | B3 | 132 | 128 | 1.03 | 1.00 | 3.1 |
| Hybrid laminates with basalt fibers in the outer and inner layers | B4 | 221 | 202 | 1.73 | 1.58 | 9.4 |
| | B5 | 216 | 198 | 1.69 | 1.55 | 9.1 |

the matrix ignition test was between 35% - 38%. In the FE modelling the properties of the unidirectional lamina was calculated using the rule of mixtures of composite materials and the fiber volume fraction was assumed to be 38% for all laminates. A variation in the fiber volume fractions between the real specimen and the modelled one will result in the variation of the critical buckling load between the two methods.

## Conclusions

The effect of fiber orientation on the critical buckling load of symmetric basalt-carbon/epoxy composite laminates was investigated using numerical nonlinear FEA method. Hybrid stacking sequences that are commonly used in wind turbine blades were studied experimentally and numerically. The specimens were subjected to simply supported boundary conditions and axial compressive load. Nonlinear numerical results had a good agreement with the experimental results. The outer layer plays the most significant role in the load carrying capability of the composite laminate. Laminates with 0° fiber orientation on the outer layer sustain higher buckling loads. Placement of carbon fiber reinforced layers on the outer surface of basalt-carbon hybrid laminates results in higher buckling strength.

## Acknowledgement

The author would like to thank the Malaysian Ministry of Higher Education for providing the financial assistance for this work through Fundamental Research Grant Scheme (FRGS), Cost Center: 0153AB-I64.

## References

1 Kaw A K, *Mechanics of Composite Materials,* (Boca Raton), 2006.
2 Mengal A N, Karuppanan S & Wahab A A, *Adv Mater Res*, 970 (2014) 67-73.
3 Khalili S M R, Daghigh V & Farsani R E, *J Reinforced Plast Compos*, 30(8) (2011) 647-659.
4 Burgoyne C J, Taranu N, Pilakoutas K, Serbescu A, Tamuzs V & Weber A, *FIB Tech Report, Stuttgart*, (2007).
5 Velde V D, Kiekens P & Langenhove V L, *Proc 10th Int Conf Composites/Nano Engineering,* USA, 2003.
6 Wang M, Zhang Z, Li Y, Li M & Sun Z, *J Reinforced Plast Compos*, 27 (2008) 393-407.
7 Cziga´ny T, *Compos Sci Technol*, 66 (2006) 3210-3223.
8 Lopresto V, Leone C & De Iorio I, *Compos Part B: Eng*, 42 (2011) 717-723.
9 Baz A & Chen T, *Proc SPIE, Active Materials and Smart Structures*, (1995), p.30-48.
10 Demirci M T, Necmettin T, Ahmet A & Ömer F E, *Compos Part B: Eng*, 66 (2014) 7-14.
11 Farsani R E, Khalili S M R & Daghigh V, *Int J Damage Mech*, 23(6) (2014) 729-744.
12 Thompson S P & Loughlan J, *Compos Struct*, 38(1) (1997) 667-678.
13 Ro J & Baz A, *Compos Eng*, 5(1) (1995) 77-90.
14 Shukla K K, Nath Y, Kreuzer E & Sateesh Kumar K V, *J Aerospace Eng*, 18(4) (2005) 215-223.
15 Topal U & Uzman U, *Mater Des*, 30(3) (2009) 710-717.
16 Yeter E, Erkliğ A & Bulut M, *Compos Struct*, 118 (2014) 19-27.
17 Erkliğ A, Yeter E & Bulut M, *Compos Struct*, 104 **(**2013) 54-59.
18 Jadhav M M & Gunjavate P V, *Int J Adv Eng Res*, 2 (1) (2012) 144-147.
19 Chikhradze N M, Marquis F D, Japaridze L A, Abashidze G S & Okujava L M, *Mater Sci Forum*, 654 (2010) 2612-2615.
20 Zhang Y, Yu C, Chu P K, Lv F, Zhang C & Ji J, *Mater Chem Phys*, 133 (2012) 845-849.
21 Khalili A, Samaratunga D, Jha R & Gopalakrishnan S, *Proc Am Soc Composites, 29th Tech Conf Composite Materials,* San Diego, CA, 2014.
22 Khalili A, Samaratunga D, Jha R, Lacy T E & Gopalakrishnan S, *23rd AIAA/ASME/AHS Adapt Struct Conf*, Kissimmee, FL, (2015) 1–11.
23 Khalili A, Samaratunga D, Jha R, Lacy T E & Gopalakrishnan S, *30th ASC Tech Conf, East Lansing,* (DEStech Publications, Inc., MI), 2015.
24 Gal E, Levy R, Abramovich H & Pavsner P, *Compos Struct*, 73(2) (2006) 179-185.
25 Muameleci M, *Master's Thesis*, Division of Solid Mechanics, Department of Management and Engineering, Linköping University, (2014) 24-72.
26 Aslan M & Sahin M, *Compos Struct*, 89 (2009) 382-390.
27 Hwang S F & Liu G H, *Compos Struct*, 53 (2001) 235-243.
28 Kilardj M, Ikhenazen G & Messager T, *J Mech Sci Technol*, 30 (2016) 3607.
29 *ANSYS procedures: Structural analysis guide*, Swanson Analysis System, 1993,
30 Jawad K O, Emad S A & Alaa A M, *Basrah J Eng Sci*, 14(2) (2014) 176-188.
31 Pineda E, Meyers D, Kosareo D, Zalewski B & Dixon G, *NASA/TM, 217822/ Part 1*, 2013.